Salecker-Wigner-Peres quantum clock applied to strong-field tunnel ionization

Nicolas Teeny,* Christoph H. Keitel, and Heiko Bauke†
Max-Planck-Institut für Kernphysik, Saupfercheckweg 1, 69117 Heidelberg, Germany

The Salecker-Wigner-Peres quantum-clock approach is applied in order to determine the tunneling time of an electron in strong-field tunnel ionization via a time-dependent electric field. Our results show that the ionization of the electron takes a nonvanishing period of time. This tunneling time is of the order of the Keldysh time but strictly larger than the Keldysh time. Comparing the quantum-clock tunneling time to the mean tunneling time as obtained by the virtual-detector approach, one finds that these two complementary methods give very similar results. Due to the asymmetric distribution of the tunneling time, there is a nonnegligible discrepancy between the mean tunneling time and the most probable tunneling time.

arXiv:1608.02854v1 [quant-ph] 9 Aug 2016

1. Introduction

Tunneling and tunnel ionization are fundamental processes in quantum mechanics, which are not only of theoretical interest but are also the foundation of some technical applications. A respectable stock of scientific works has been devoted to this topic. Nevertheless, some aspects of tunneling are discussed controversially till today, in particular the temporal development of the tunneling dynamics and the time span that is required to cross the tunneling barrier. The issue of tunneling times was first considered by MacColl in Ref. [1] for a free particle tunneling through a static square potential. In this case, a particle approaches from far away a potential wall higher than its initial kinetic energy. Since MacColl's pioneering work many approaches and methods have been proposed to define a tunneling time [2, 3] for this physical situation, which can be classified into three categories.

A possible and very intuitive approach is to determine the traversal time by following the center of gravity of the transmitted wave packet [4]. The associated time, however, has little physical significance as argued in Ref. [3]. The second class of approaches constructs a set of dynamical paths and determines how much time each path spends under the tunneling barrier. Then, one can define the most probable time spent under the barrier, corresponding to the most probable path, or an average time spent under the barrier by taking a weighted average over all paths. Among others, this approach is realized by the Bohm method as described in Refs. [5, 6] and references therein, the Feynman path integrals method as applied in Refs. [6–8], and finally the Wigner distribution paths method as studied in Refs. [9–11]. Time is not only a coordinate of the universal space-time background where physical processes take place. Time can also be introduced as a dynamical variable of physical systems that clock a certain process [12], which leads us to the third category of approaches to define a tunneling time. In the so-called quantum-clock approach, an additional physical system is coupled to the system which undergoes the tunneling dynamics [13–18]. Then either a dynamical variable of the coupled system acts as a clock or the accessory system has an explicit time dependence with a given time scale, which provides a reference for time measurements [19, 20]. Depending on how temporal quantities are extracted from the clock system, the quantum-clock approach gives rise to definitions of various times which characterize the tunneling dynamics, e. g., the dwell time, the tunneling (traversal) time, or the reflection time.

Early works on tunnling times mainly focus on tunneling prosesses where an asymptotically free particle approaches a static potential barrier, tunnels though the barrier, and finally becomes free again. Currently, the issue of tunnel ionization times got into the focus of scientific research due to the progress in experimental atomic physics, which allows one to probe strong-field ionization dynamics at attosecond time scales [21, 22]. These experiments are often referred to as attoclock experiments. Tunneling of initially free particles is quite different from tunnel ionization [23, 24] in atomic physics. Here, the particle is initially bound by a binding potential and then excited by a time-dependent electric field pulse which induces the tunneling dynamics. Because the typical time scale of the driving electric field is large compared to the typical tunneling time, the electron's wave function has time to adapt to the changing potential barrier. Since these attoclock experiments have been performed, many renewed efforts have been directed toward defining a tunnel ionization time because a consensus on a suitable theoretical definition of tunneling time and the interpretation of experimental results is still lacking [21–39].

For studying tunneling times in tunnel ionization theoretically, many approaches can be adopted from tunneling of initially free particles. For example, the Wigner time approach [7, 40, 41] was applied to tunnel ionization in the adiabatic limit in Refs. [27, 33]. The adiabatic limit corresponds to a parameter regime where the time scale of the tunneling dynamics is short compared to the time scale of the variation of the electric field. Calculating the complex transmission amplitude as a function of the barrier height and the electron energy, various theoretical definitions of tunneling times can be introduced, often referred to as Büttiker-Landauer time, Pollack-Miller time, Eisenbud-Wigner time, and Lamor time. These have been compared to experimental results in Refs. [32, 42]. The interpretation of the attoclock measurements is, however, not trivial and depends on the employed theoretical model of the ionization dynamics [36]. It is a commonly applied assumption that ionization happens at the instant of the electric field maximum. It has, however, been shown recently by applying the virtual-detector approach to

* nicolas.teeny@mpi-hd.mpg.de
† heiko.bauke@mpi-hd.mpg.de

strong-field tunnel ionization in Refs. [38, 39] that the moment when the electron leaves the tunneling barrier does not necessarily coincide with the moment of electric field maximum.

Except the virtual-detector approach, none of the above mentioned approaches has been applied to tunnel ionization in a time-dependent potential, i. e., taking into account the continuous increase and decay of the external driving electric field as it is the situation in an experimental setting. Often the external field is treated as static [33] or switched on instantaneously [23, 24]. As emphasized in Ref. [24], tunneling in a continuously evolving potential is very different from the sudden turn-on case. In particular, in a slowly varying electric field there is no natural reference point in time which defines when tunneling begins. Furthermore, the quantum state at the onset of tunneling is no longer the ground state of the unperturbed binding potential. When tunneling sets in, the wave function has already evolved in the time-dependent potential.

In this work, we apply the Salecker-Wigner-Peres quantum clock to strong-field tunnel ionization taking into account the continuous evolution of the driving electric field to determine the the dwell time, the traversal time, and the reflection time. The obtained traversal time is compared to the mean tunneling time as calculated by the recently developed virtual-detector method [38, 39]. The article is organized as follows: In Sec. 2, the considered system is described. The Salecker-Wigner-Peres quantum clock is reviewed in Sec. 3, before we explain how to apply this approach to determine the tunneling time of tunnel ionization. Our main results are presented and interpreted in Sec. 4. In Sec. 5 finally, we summarize our main results.

2. Tunnel ionization from a two-dimensional Coulomb potential

In the following, we will study tunnel ionization from a two-dimensional Coulomb potential induced via a driving homogenous electric field. This two-dimensional system resembles tunnel ionization from hydrogen-like ions while keeping the computational demands small. In the long-wavelength limit, i. e., when the dipole approximation is applicable, the three-dimensional Coulomb potential with an external electric field has rotational symmetry around the electric field direction, which makes this system quasi two-dimensional.

Choosing the coordinate system such that the linearly polarized external electric field with the amplitude $\mathcal{E}(t)$ points into the x direction, the Schrödinger equation for the Coulomb problem with the Hamiltonian $\hat{H}_E$ reads

$$\mathrm{i}\hbar\frac{\partial\Psi(x,y,t)}{\partial t} = \hat{H}_E\Psi(x,y,t) = \left(-\frac{\hbar^2}{2m}\left(\frac{\partial^2}{\partial x^2}+\frac{\partial^2}{\partial y^2}\right) - \frac{Ze^2}{4\pi\varepsilon_0\sqrt{x^2+y^2}} - ex\mathcal{E}(t)\right)\Psi(x,y,t)\,. \tag{1}$$

Here m, e, Z, and ε_0 denote the electron's mass, the elementary charge, the atom's atomic number, and the vacuum permittivity, respectively. Applying an electric field pulse with a unique maximum allows us to study the ionization dynamics without undesirable artifacts, i. e., to avoid multiple ionization and rescattering. Therefore, we employ a Gaussian pulse, i. e., the electric field is given by

$$\mathcal{E}(t) = \mathcal{E}_0\exp\left(-\tfrac{\omega_\mathcal{E}^2(t-t_0)^2}{2}\right). \tag{2}$$

The time t_0 denotes the instant of maximal electric field $\mathcal{E}_0$ and $\tau_\mathcal{E} = \sqrt{2}/\omega_\mathcal{E}$ is the time scale of the raise and decay of the electric field. Note that at $t \approx t_0$ the Gaussian pulse (2) corresponds approximately to a sinusoidal pulse with $\mathcal{E}(t) = \mathcal{E}_0\cos(\omega_\mathcal{E} t)$.

3. Salecker-Wigner-Peres quantum clock

3.1. Fundamentals

Salecker, Wigner, and Peres [13, 16] introduced a quantum system that can serve as a clock, the so-called Salecker-Wigner-Peres quantum clock. This clock system is characterized by the Hamiltonian $\hat{H}_c = \omega\hat{J}$, where $\hat{J} = -\mathrm{i}\hbar\frac{\partial}{\partial\theta}$ denotes an angular momentum operator for the angular coordinate θ and ω is an angular frequency. Obviously, the operators $\hat{H}_c$ and $\hat{J}$ share a common set of eigen-functions. Restricting the angular variable θ to $\theta \in [0, 2\pi)$ and imposing periodic boundary conditions, the clock Hamiltonian $\hat{H}_c$ and the operator $\hat{J}$ possess the equidistant discrete spectra $n\hbar\omega$ and $n\hbar$, respectively, with integer n. The corresponding normalized eigen-functions will be denoted by $|J_n\rangle$ in the following.

For the subspace that is spanned by the orthonormal functions $|J_{-j}\rangle, \ldots, |J_j\rangle$ the following new basis set can be introduced:

$$|V_k\rangle = \frac{1}{\sqrt{N}}\sum_{n=-j}^{j}\exp\left(-\tfrac{2\pi\mathrm{i}kn}{N}\right)|J_n\rangle\,, \tag{3}$$

with $N = 2j+1$ and $k = 0, 1, \ldots, N-1$. The N states $|V_k\rangle$ are called clock states. Under the evolution of the clock Hamiltonian, an initial clock state cycles successively through all clock states. A short calculations shows for $\Delta t = 2\pi/(N\omega)$

$$\exp\left(-\tfrac{\mathrm{i}\hat{H}_c\Delta t}{\hbar}\right)|V_k\rangle = \frac{1}{\sqrt{N}}\sum_{n=-j}^{j}\exp\left(-\tfrac{2\pi\mathrm{i}n}{N}\right)\exp\left(-\tfrac{2\pi\mathrm{i}kn}{N}\right)|J_n\rangle = |V_{(k+1)\bmod N}\rangle\,. \tag{4}$$

This means, after preparing $|V_0\rangle$ as the clock's initial state, the clock's quantum state passes trough $|V_0\rangle$, $|V_1\rangle$, $|V_2\rangle$, and so on at times $t = 0$, $t = \Delta t$, $t = 2\,\Delta t$, and so on until $|V_{N-1}\rangle$ passes into $|V_0\rangle$ after a further time step of Δt.

Introducing the set of projection operators $\hat{P}_k$ which fulfill

$$\hat{P}_k|V_l\rangle = \left(|V_k\rangle\langle V_k|\right)|V_l\rangle = \delta_{k,l}|V_k\rangle \tag{5}$$

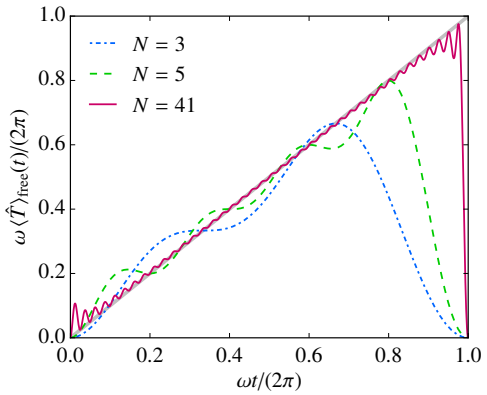

FIG. 1: Expectation value of the clock operator $\langle\hat{T}\rangle = f(t)$ as a function of time t for freely running clocks with different numbers of clock states N and $|V_0\rangle$ as the initial quantum state. As a reference, the solid gray line indicates linear passage of time.

for $k, l = 0, 1, \ldots, N-1$, one can define the clock operator

$$\hat{T} = \sum_{k=0}^{N-1} \Delta t\, k \hat{P}_k \,. \tag{6}$$

The time-dependent expectation value of the operator (6) for a free-running clock with $|V_0\rangle$ as its initial state

$$\langle\hat{T}\rangle_{\text{free}}(t) = \left\langle V_0 \left| \exp\left(\tfrac{\mathrm{i}\hat{H}_c t}{\hbar}\right)\hat{T}\exp\left(-\tfrac{\mathrm{i}\hat{H}_c t}{\hbar}\right)\right| V_0\right\rangle \tag{7}$$

equals at times $t = n\,\Delta t$

$$\langle\hat{T}(n\,\Delta t)\rangle_{\text{free}} = \left\langle V_{n \bmod N}\left|\hat{T}\right|V_{n \bmod N}\right\rangle = \Delta t\,(n \bmod N)\,, \tag{8}$$

as a consequences of Eq. (4). The expectation value (7) is shown in Fig. 1 as a function of time t and different numbers of clock states N. As seen in this figure, for noninterger multiples of Δt, the expectation value of the clock operator deviates from the laboratory time t. Thus, the quantity Δt characterizes the resolution of the quantum clock. In particular at $t \gtrapprox 0$ and $t \lessapprox 2\pi/\omega = N\,\Delta t$, the periodicity of the clock operator induces large oscillations near the clock's discontinuity at $t = N\,\Delta t$ similar to the Gibbs-Wilbraham phenomenon [43].

3.2. Coupling the Salecker-Wigner-Peres quantum clock to a dynamical system

In order to measure the duration of a dynamical process in some quantum system with the Hamiltonian $\hat{H}$, the Salecker-Wigner-Peres quantum clock has to be coupled to the system of interest. The Hilbert space of the combined system with the Hamiltonian $\hat{H}_T$ becomes the tensor product of the Hilbert space of $\hat{H}$ with the state vector $|\Psi\rangle$ and of the clock Hamiltonian $\hat{H}_c$ with the state vector $|\Psi_c\rangle$. Thus, the quantum state of the combined system becomes $|\Phi\rangle = |\Psi\rangle \otimes |\Psi_c\rangle$, which may be represented by an N-component wave function in case of a N-level clock system. To give a specific example, let us consider the time of flight of a free particle of mass m [16, 44] in one dimension. In this case, the one-dimensional Hamiltonian $\hat{H}$ coupled to a clock Hamiltonian $\hat{H}_c$ with $N = 2j + 1$ states is given by [16]

$$\hat{H}_T = \hat{H} + \hat{P}([0,\ell])\hat{H}_c = \\ -\frac{\hbar^2}{2m}\frac{\mathrm{d}^2}{\mathrm{d}x^2} + \hat{P}([0,\ell])\hbar\omega \begin{pmatrix} j & & & \\ & j-1 & & \\ & & \ddots & \\ & & & -j \end{pmatrix}. \tag{9}$$

Here, $\hat{H}_c$ is represented in its eigen-basis and $\hat{P}([0,\ell])$ denotes the projection operator on $x \in [0,\ell]$, which is the region of the time-of-flight measurement. This operator yields one for $x \in [0,\ell]$ and zero otherwise. Using the Hamiltonian (9), one is able to measure how much time the free particle spends in the region $x \in [0,\ell]$ because the coupling of the wave function to the clock Hamiltonian $\hat{H}_c$ is restricted to this range. To determine the time of flight, the state $|\Psi_0\rangle \otimes |V_0\rangle$ is prepared as the initial condition, such that $|\Psi_0\rangle$ represents a particle far away from $[0,\ell]$. The the time operator (6) is applied to the evolving quantum state $|\Phi\rangle$ of the combined system.

Figure 1 shows that for large N, the expectation value of the clock operator follows closely the laboratory time t, in particular at $t \approx \pi/\omega$. Nevertheless, it is not desirable to choose a large number of clock states N because the extraneous disturbance of the quantum system due to the clock Hamiltonian is also proportional to N. In order not to disturb the quantum system under investigation by the clock Hamiltonian, we set $N = 3$ in the following. For $N = 3$, the clock operator's expectation value grows monotonously with time t, at least for $t \in [0, 2\,\Delta t]$. Thus, we can invert the function $\langle\hat{T}\rangle_{\text{free}}(t)$, which yields the expectation value of the operator (6) of a free running clock, to calibrate the quantum clock [44]. In this way, the laboratory time t can be inferred from the clock operator's expectation value to much higher accuracy than given by Δt.

3.3. Determining tunneling times in tunnel ionization

In tunnel ionization of an electron initially bound to a Coulomb potential, the space can be divided in to a classically allowed region and a classically forbidden region, which also contains the tunneling region. The shape of the tunneling region is formed by bending the atomic binding potential via the applied external electric field and the electron's ground-state energy corrected by Stark-shift effects; see Fig. 2 and Ref. [39] for details. Introducing the parabolic coordinates ξ and η via

$$x = \frac{\xi - \eta}{2}\,, \qquad\qquad y = \sqrt{\xi\eta}\,, \tag{10}$$

the tunneling region is confined by lines of constant ξ and η. In order to measure the tunneling ionization time by the quantum clock, the coupling between the quantum clock and the electron is established in the tunneling barrier region $\mathcal{B}$ via the projection

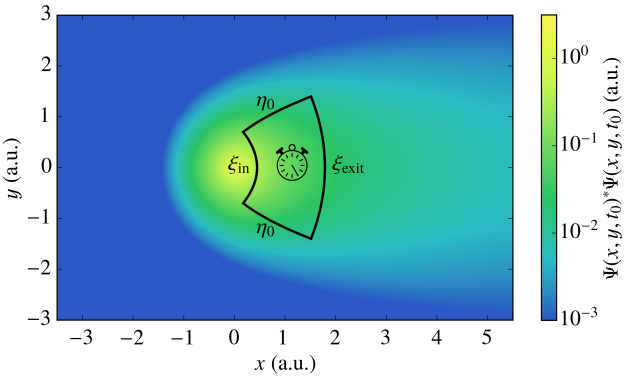

FIG. 2: Schematic of tunneling time determination in strong-field ionization via the Salecker-Wigner-Peres quantum clock. The coupling of the clock's Hamiltonian to electron's Hamiltonian is established in the tunneling barrier region $\mathcal{B}$ between the lines $\eta = \eta_0$, $\xi = \xi_{\text{in}}$ and $\xi = \xi_{\text{exit}}$ indicated by the black solid lines; see Ref. [39]. The wave function's probability density $|\Psi(x, y, t)|^2$ at the instant of electric field maximum, i. e., at $t = t_0$, is represented by colors for $\mathcal{E}_0 = 1.1$ a.u., $Z = 1$, and $\gamma = 0.25$.

operator $\hat{P}(\mathcal{B})$. Thus, the corresponding Hamiltonian is given by

$$\hat{H}_T = \hat{H}_E + \hat{P}(\mathcal{B})\hat{H}_c\,, \tag{11}$$

where $\hat{H}_E$ is the electron Hamiltonian as defined in Eq. (1) and $\hat{H}_c$ denotes an N-level clock Hamiltonian with $N = 2j + 1 = 3$. The combined wave function $|\Phi(t)\rangle$ of the electron and the clock is initially given by $|\Phi(0)\rangle = |\Psi_0\rangle \otimes |V_0\rangle$, where $|\Psi_0\rangle$ denotes the ground state of the two-dimensional Coulomb potential.

In general, the tunneling region is time-dependent due to the time-dependent electric field (2). Nevertheless, we consider a time-independent tunneling region which is given for the peak of the applied electric field at time $t = t_0$. Coupling the quantum clock to the electron in this fixed tunneling region is justified because for static fields the tunneling probability is maximal for maximal electric fields and it is exponentially suppressed for lower fields.

The projection operator $\hat{P}(\mathcal{B})$ in Eq. (11) is designed to advance the quantum clock only when the electron is in the tunneling region. However, the determination of the tunneling time via the quantum clock is complicated by the fact that there is always a small portion of the electron wave packet in the tunneling region even at a vanishing electric field, i. e., before the tunneling dynamics starts. Moreover, only a part of the probability density which enters the tunneling region will eventually escape the tunneling region and become free. The other part gets just reflected under the tunneling barrier. Since the quantum clock cannot differentiate between the reflected and the tunneled part of the electron wave packet, it determines the time spent in the tunneling barrier region $\mathcal{B}$ irrespective whether the electron is eventually reflected or transmitted. This time is known as the dwell time (or sojourn time) $\tilde{\tau}_D$ and was discriminated clearly from other concepts of tunneling times for the first time by Büttiker [17]. The following alternative expression

$$\tau'_D = \int_0^\infty \int_{\mathcal{B}} |\Psi(x, y, t)|^2 \,\mathrm{d}x\,\mathrm{d}y\,\mathrm{d}t \tag{12}$$

for the dwell time can be derived within conventional [7] as well as within Bohm's [45] interpretations of quantum mechanics and is commonly accepted by now [46].

The tunneling time can be derived from the dwell time or the asymptotic expectation value of the clock operator (6) applied to the wave function $|\Phi\rangle$, respectively, via splitting this time into a weighted sum of a tunneling time $\tilde{\tau}_T$ and a reflection time $\tilde{\tau}_R$ as shown in the following. After the tunneling dynamics has finished, the quantum state $|\Phi\rangle$ can be separated into a bound part $|\Phi_{\text{bound}}\rangle$ and a free part $|\Phi_{\text{free}}\rangle$ which both occupy two disjunct space regions. Such regions may be defined via a sphere of sufficiently large radius around the atomic core, which disjoins both regions. Thus, the quantum state $|\Phi\rangle$ after the interaction with the driving electric field, can be written as a superposition of the two orthonormal states $|\Phi_{\text{bound}}\rangle$ and $|\Phi_{\text{free}}\rangle$ as

$$|\Phi\rangle = \sqrt{T}\;|\Phi_{\text{free}}\rangle + \sqrt{R}\;|\Phi_{\text{bound}}\rangle\,, \tag{13}$$

where T denotes the total tunneling probability and R is the deflection probability with $1 = T + R$. Consequently, the asymptotic expectation value of the clock operator

$$\lim_{t\to\infty} \left\langle \Phi(t) \middle| \hat{T} \middle| \Phi(t) \right\rangle = \left\langle \Phi \middle| \hat{T} \middle| \Phi \right\rangle = \tilde{\tau}_D \tag{14}$$

may be written as

$$\tilde{\tau}_D = T\tilde{\tau}_T + R\tilde{\tau}_R\,, \tag{15}$$

where we have introduced the (not calibrated) tunneling time

$$\tilde{\tau}_T = \left\langle \Phi_{\text{free}} \middle| \hat{T} \middle| \Phi_{\text{free}} \right\rangle \tag{16a}$$

and the (not calibrated) reflection time

$$\tilde{\tau}_R = \left\langle \Phi_{\text{bound}} \middle| \hat{T} \middle| \Phi_{\text{bound}} \right\rangle . \tag{16b}$$

The time $\tilde{\tau}_D$ but also $\tilde{\tau}_T$ and $\tilde{\tau}_R$ do not grow proportionally to the laboratory time t. For example, the physical dwell time is related to $\tilde{\tau}_D$ via $\tilde{\tau}_D = \langle \hat{T} \rangle_{\text{free}}(\tau_D)$, as noted in Sec. 3.2. Thus, the expectation values $\tilde{\tau}_D$, $\tilde{\tau}_T$, and $\tilde{\tau}_R$ have to be corrected via inverting $\langle \hat{T} \rangle_{\text{free}}(t)$ to get the physical dwell, tunneling, and reflection times

$$\tau_D = \overline{\langle \hat{T} \rangle_{\text{free}}}(\tilde{\tau}_D)\,, \tag{17}$$

$$\tau_T = \overline{\langle \hat{T} \rangle_{\text{free}}}(\tilde{\tau}_T)\,, \tag{18}$$

$$\tau_R = \overline{\langle \hat{T} \rangle_{\text{free}}}(\tilde{\tau}_R)\,, \tag{19}$$

where the bar indicates the function's inverse.

Although the splitting (15) has been employed in many works [47, 48], it has also been criticized [3, 49, 50]. One point of criticism that was put forward is that the dwell time

(12) adds up probability density rather than probability amplitudes and therefore neglects possible interferences between transmitted and reflected portions of the electron's wave packet. This argument, however, does not apply to the clock approach taken here. The clock Hamiltonian couples to the wave function, not to the density. Furthermore, the expectation value (15) is calculated when the tunneled and the bound parts of the wave function are well separated and therefore there is no interference between both parts. For the quantum-clock approach it is not required to separate the wave function into tunneling and reflecting parts under the barrier, which would be problematic indeed.

4. Numerical results and interpretation

4.1. Dwell time, tunneling time, and reflection time

After having specified the theoretical foundations of our quantum-clock approach to tunnel ionization in the previous sections, we can present the numerical results as obtained by solving the Schrödinger equation with the Hamiltonian (11) numerically, see the Appendix for details regarding the numerical methods. The so-called Keldysh parameter $\gamma = \omega_\mathcal{E} \sqrt{-2E_E m}/(e\mathcal{E}_0)$ [25] characterizes the ionization process as dominated by tunneling for $\gamma \ll 1$ or by multiphoton ionization for $\gamma \gg 1$. Here, E_E denotes the ground state binding energy, which equals $E_E = -2Z^2$ a.u. for the two-dimensional Coulomb problem [51]. In the following, the electric field amplitude $\mathcal{E}_0$ and the frequency $\omega_\mathcal{E}$ are adjusted such that $\gamma = 0.25 < 1$. The clock parameters $\Delta t = 200/Z^2$ a.u. and $N = 3$ are chosen such that $|j\hbar\omega/E_E| = 0.0104 \ll 1$, i. e., the quantum clock Hamiltonian is coupled weakly to the electron's ave function. This ensures that the perturbation of the

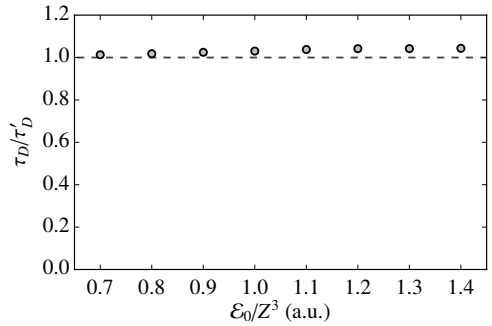

FIG. 3: The ratio of the dwell time τ'_D determined by integrating the probability density in the tunneling barrier to the (corrected) dwell time τ_D as given by the quantum clock for different electric field strengths $\mathcal{E}_0$ and for a constant Keldysh parameter $\gamma = 0.25$. To guide the eye, the horizontal dashed line indicates the ratio one, i. e., when both dwell times exactly agree.

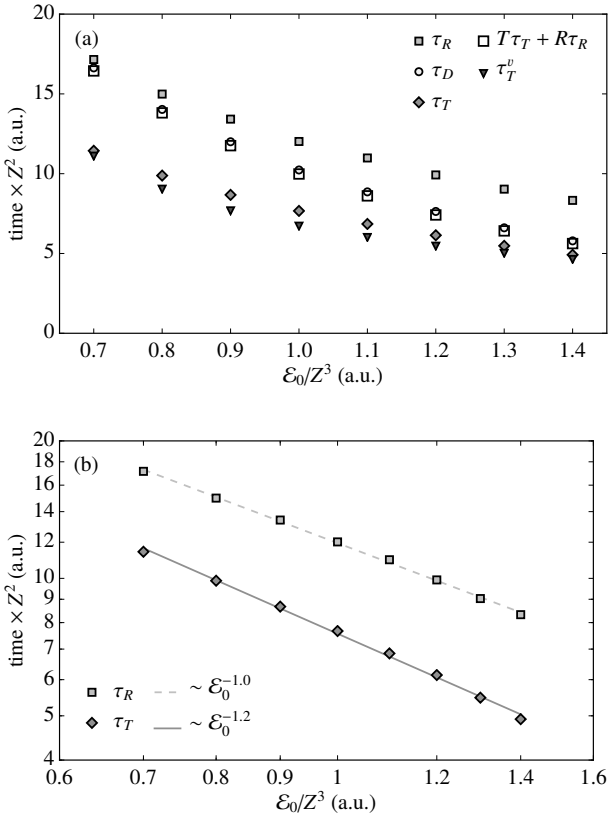

FIG. 4: (a): Reflection time τ_R, dwell time τ_D, tunneling time τ_T, the weighted sum $T\tau_T + R\tau_R$, and tunneling time τ_T^v for different electric field strengths $\mathcal{E}_0$ at a fixed Keldysh parameter $\gamma = 0.25$. (b): Reflection time τ_R and tunneling time of subfigure (a) on a double logarithmic scale. For specific definitions of the various times see the main text.

Coulomb Hamiltonian $\hat{H}_E$ by the quantum clock Hamiltonian $\hat{H}_c$ is negligible. This has been tested by repeating numerical calculations with $\Delta t = 400/Z^2$ a.u., i. e., even weaker coupling, which yields results that agree with the results obtained for $\Delta t = 200/Z^2$ a.u. up to small numerical discrepancies. Note that choosing the clock parameter Δt arbitrarily large such that the influence of the clock on the studied system becomes arbitrarily small leads to numerical difficulties. With very small Δt also transitions between various clock states $|V_k\rangle$ become small and therefore difficult to resolve numerically. As explained in Sec. 3.2 increasing the number of states of the clock system does not improve the clock precision, and thus we choose the smallest nontrivial odd number of states $N = 3$. A larger number of states N would increase the required numerical effort without providing any advantage.

The two definitions of the dwell time (12) and (17), respectively, provide us a valuable consistency check of the quantum-clock approach. To be consistent, the dwell time as determined by the quantum clock (17) must agree with the dwell time (12), which does not rely on the concept of a quantum clock. Our numerical results shown in Fig. 3 confirm this property. For the chosen parameters, both dwell times agree up to a discrepancy of about 4 %. For larger field strengths $\mathcal{E}_0$ this small

discrepancy tends to be systematically larger than for small field strengths. This can be attributed to the fact that the dwell time becomes small for large field strengths and therefore the relative accuracy of the dwell-time determination is reduced.

The tunneling time τ_T, the reflection time τ_R, as well as the dwell time τ_D are presented in Fig. 4(a). Furthermore, the figure shows the weighted sum $T\tau_T + R\tau_R$, which is close to the dwell time τ_D. But in contrast to the relation (15), $T\tau_T + R\tau_R$ does not strictly agree with τ_D due to the nonlinearity of the function $\langle\hat{T}\rangle_{\text{free}}(t)$. Because τ_D equals approximately the weighted average $T\tau_T + R\tau_R$, the dwell time τ_D lies always between the tunneling time τ_T and the reflection time τ_R. For the in Fig. 4 considered parameter range, the reflection time τ_R is larger than the tunneling time τ_T by a factor of approximately 1.6. This can be intuitively understood as tunneling electrons enter the barrier and then leave the barrier at the exit while reflected electrons move under the barrier until they get reflected at the barrier exit and then travel back into the direction of the atomic core. The tunneling time as well as the reflection time decrease with increasing electric field strength $\mathcal{E}_0$. In fact, we find a power-law behavior for τ_T as well as for τ_R, $\tau_T \sim \mathcal{E}_0^{-1.2}$ and $\tau_R \sim \mathcal{E}_0^{-1}$ as shown in 4(b). This scaling behavior is similar to the scaling of the Keldysh time $\tau_K = \sqrt{-2E_E m}/(e\mathcal{E}_0)$, which has been identified as a lower bound for the tunneling time in ionization by an instantaneously turned on field [28, 52]. In fact, the Keldysh time is always smaller than the tunneling time τ_T by a factor of about four for the parameter range of Fig. 4.

4.2. Relation to the virtual-detector approach

In Ref. [39], we studied tunneling times for the same kind of system and the same parameter regime as in this article by a different approach, the so-called virtual-detector method. It is the purpose of this section to relate the virtual-detector approach to the quantum-clock approach. We are going to demonstrate that both complementary methods give compatible results for the tunneling time in strong-field ionization.

The central idea of the virtual-detector approach is to determine the electron's probability density flow at the entry line and the exit line of the tunneling barrier at the parabolic coordinates $\xi = \xi_{\text{in}}$ and $\xi = \xi_{\text{exit}}$ as functions of the time t. Integrating the probability density flow along these lines gives the quantities $D\xi_{\text{in}}(t)$ and $D\xi_{\text{exit}}(t)$. Furthermore, $D_{\xi_{\text{in}}}(t)\,\Theta(D_{\xi_{\text{in}}}(t))\,\Delta t$ is proportional to the probability that the electron crosses during the short time interval $[t, t+\Delta t]$ the entry line of the tunneling barrier into the direction away from the atomic core. Here $\Theta(x)$ denotes the Heaviside step function. Similarly, $D_{\xi_{\text{exit}}}(t)\,\Theta(D_{\xi_{\text{exit}}}(t))\,\Delta t$ is proportional to the probability that the electron crosses the exit line of the tunneling barrier into the direction away from the atomic core. It is convenient to introduce the normalization constants N_{in} and N_{exit} and the distributions $p_{\text{in}}(t)$ and $p_{\text{exit}}(t)$ such that

$$p_{\text{in}}(t) = \frac{1}{N_{\text{in}}} D_{\xi_{\text{in}}}(t)\,\Theta(D_{\xi_{\text{in}}}(t))\,, \tag{20a}$$

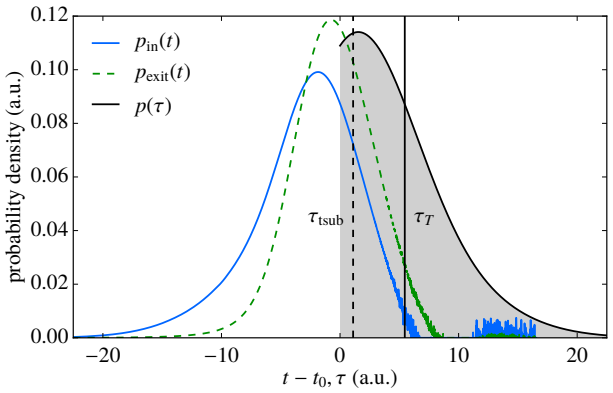

FIG. 5: Probability distributions $p_{\text{in}}(t)$ and $p_{\text{exit}}(t)$ to enter or to leave the tunneling barrier into the direction away from the atomic core as functions of time and the probability distribution $p(\tau)$ of the tunneling time as derived from $p_{\text{in}}(t)$ and $p_{\text{exit}}(t)$ for $\mathcal{E}_0 = 1.2$ a.u. and $Z = 1$. The vertical black dashed line indicates the time τ_{tsub}, which is the distance of the positions of the maxima of the distributions $p_{\text{in}}(t)$ and $p_{\text{exit}}(t)$. The vertical black solid line corresponds to the tunneling time τ_T.

$$p_{\text{exit}}(t) = \frac{1}{N_{\text{exit}}} D_{\xi_{\text{exit}}}(t)\,\Theta(D_{\xi_{\text{exit}}}(t))\,, \tag{20b}$$

and

$$\int_{-\infty}^{\infty} p_{\text{in}}(t)\,\mathrm{d}t = 1\,, \tag{21a}$$

$$\int_{-\infty}^{\infty} p_{\text{exit}}(t)\,\mathrm{d}t = 1\,. \tag{21b}$$

The functions $D_{\xi_{\text{in}}}(t)$ and $D_{\xi_{\text{exit}}}(t)$ have both a unique global maximum; see Fig. 5. In Ref. [39], we defined the distance of the positions of these maxima as the tunneling time τ_{tsub}, which was also determined numerically for the same parameters as in this article.

Comparing τ_{tsub} and τ_T, one finds that τ_{tsub} is smaller than τ_T by a factor of about three. This discrepancy is a direct consequence of the different definitions of τ_{tsub} and τ_T. It does not necessarily indicate a conflict between the quantum-clock approach and the virtual-detector approach. As we will show in the following, the discrepancy arises essentially because taking the difference between two expectation values of two times is not equivalent to determining the expectation value of a time delay. Due to the approximate symmetry of $p_{\text{in}}(t)$ and $p_{\text{exit}}(t)$ around their maxima, τ_{tsub} equals approximately the difference between the expectation values for the moments of entering and leaving the tunneling barrier. The tunneling time τ_T, however, is derived from an expectation value of a clock operator which determines directly the time spend in the tunneling barrier. As a quantum mechanical observable, the time that corresponds to this operator has some intrinsic distribution. Neglecting possible quantum correlations between entering and leaving the tunneling barrier, one can reconstruct this distribution from $p_{\text{in}}(t)$ and $p_{\text{exit}}(t)$ by assuming that the probability to spend the nonnegative time τ in the tunneling barrier is proportional to the product of $p_{\text{in}}(t)$ at the entry time t

and $p_{\mathrm{exit}}(t+\tau)$. Integrating over all possible entry times yields then the probability distribution

$$p(\tau) = \frac{1}{N}\int_{-\infty}^{\infty} p_{\mathrm{in}}(t)p_{\mathrm{exit}}(t+\tau)\,\mathrm{d}t\,, \tag{22}$$

where N is a normalization constant such that

$$\int_0^{\infty} p(\tau)\,\mathrm{d}\tau = 1\,. \tag{23}$$

Note that due to causality reasons, $p(\tau)$ vanishes for $\tau < 0$. The corresponding expectation value of the tunneling time of the virtual-detector approach is then

$$\tau_T^v = \int_0^{\infty} \tau p(\tau)\,\mathrm{d}\tau\,. \tag{24}$$

For comparison with the tunneling time τ_T of the quantum-clock approach, the time τ_T^v is also indicated in Fig. 4(a). In contrast to tunneling delay τ_{tsub}, τ_T^v is very close to the tunneling time τ_T of the quantum-clock approach. As one can see in Fig. 5, the distribution $p(\tau)$ has a maximum approximately at τ_{tsub}. Thus, τ_{tsub} corresponds to the most probable tunneling time. Due to the distribution's asymmetry that results from the causality condition $p(\tau) = 0$ for $\tau < 0$, the expectation value of $p(\tau)$ is shifted away from the position of the maximum to larger values, which explains the factor-3 discrepancy between τ_{tsub} and τ_T.

5. Conclusions

We determined the tunneling time of strong-field tunnel ionization from a two-dimensional Coulomb potential by utilizing the Salecker-Wigner-Peres quantum clock. A mean tunneling time of the order of four times the Keldysh time was found by this method. In Refs. [28, 52], the Keldysh time was identified as the time it takes the ground state in the presence of a driving electric field to evolve into the quasistatic resonance state after an instantaneous turn-on of the field. Thus, the obtained tunneling time may be seen as an indication that the Keldysh time characterizes the time to develop quasistatic resonance state also in the case of a continuously evolving electric field.

The quantum-clock approach is complementary to the virtual-detector approach that was taken in an earlier work. The mean tunneling time as identified by the quantum clock could be reproduced from the probability distributions for the moments of entering and leaving the tunneling barrier, which were determined by the virtual-detector approach, and assuming statistical independence of entering and leaving the tunneling barrier. This has two implications. The fact that we find almost the same mean tunneling time by two very different theoretical approaches is a strong indication that in agreement with there *is* a nonzero tunneling time and tunneling is neither instantaneous nor superluminal, in agreement with experimental findings [32] and other theoretical findings, e. g., in Ref. [42]. Furthermore, the agreement of both methods may be interpreted as that entering and leaving the tunneling barrier are nearly statistically independent, up to the causality condition that the electron cannot leave the tunneling barrier before it has entered the barrier.

A substantial difference was found between the most probable tunneling time and the mean tunneling time, which is larger than the former. This may be of experimental relevance. An ideal series of experimental measurements should yield the mean tunneling time. As pointed out in Ref. [42], only a post-selected subset of ionized electrons may be actually detected, corresponding to, e. g., electrons with the most probable momentum or with the most probable tunneling time. In the latter case, an experiment would find the most probable tunneling time, not the mean tunneling time. Consequently, it is essential to distinguish between the mean tunneling time and other kinds of tunneling time when comparing tunneling times quantitatively.

A. Numerical methods

Coupling the quantum clock Hamiltonian to the electron's Schrödinger Hamiltonian yields an Hamiltonian for a N-component wave function. Because the clock Hamiltonian is diagonal, however, the resulting equation of motion for this N-component wave function separates into N independent one-component Schrödinger equations which are given by the usual Schrödinger equation for the electron modified by an additional clock potential. At least in principle, these time-dependent Schrödinger equations may be solved numerically by any standard method.

Due to the Coulomb potential's singularity and the weakness of the clock potential (compared to the Coulomb potential) a naive application of some standard method is likely to fail. Numerical difficulties in the application of the quantum-clock approach may be circumvented by employing a Trotter-Suzuki splitting scheme [53]. In this scheme, the time evolution operator of the whole quantum system is split into products of time evolution operators for the clock Hamiltonian and the Schrödinger Hamiltonian with the Coulomb potential plus the external electric field. The clock Hamiltonian can be propagated exactly. The remaining Schrödinger Hamiltonian is propagated by employing a Lanczos propagator [54, 55] and a fourth-order finite differences scheme for the discretization of the Hamilton operator.

[1] L. A. MacColl, "Note on the transmission and reflection of wave packets by potential barriers," Phys. Rev. **40**, 621 (1932).

[2] E. H. Hauge and J. A. Støvneng, "Tunneling times: a critical review," Rev. Mod. Phys. **61**, 917 (1989).

[3] R. Landauer and T. Martin, "Barrier interaction time in tunneling," Rev. Mod. Phys. **66**, 217 (1994).

[4] T. Martin and R. Landauer, "Time delay of evanescent electromagnetic waves and the analogy to particle tunneling," Phys. Rev. A **45**, 2611 (1992).

[5] C. R. Leavens and G. C. Aers, "Bohm trajectories and the tunneling time problem," in *Scanning Tunneling Microscopy III*, Springer Series in Surface Sciences, Vol. 29, edited by R. Wiesendanger and H.-J. Güntherodt (Springer, Heidelberg, 1996) pp. 105–140.

[6] C. R. Leavens, "Bohm trajectory and Feynman path approaches to the "Tunneling time problem"," Found. Phys. **25**, 229 (1995).

[7] D. Sokolovski and L. M. Baskin, "Traversal time in quantum scattering," Phys. Rev. A **36**, 4604 (1987).

[8] H. A. Fertig, "Traversal-time distribution and the uncertainty principle in quantum tunneling," Phys. Rev. Lett. **65**, 2321 (1990).

[9] K. L. Jensen and F. A. Buot, "Numerical calculation of particle trajectories and tunneling times for resonant tunneling barrier structures," Appl. Phys. Lett. **55**, 669 (1989).

[10] N. L. Balazs and A. Voros, "Wigner's function and tunneling," Ann. Phys. (N.Y.) **199**, 123 (1990).

[11] M. S. Marinov and B. Segev, "Quantum tunneling in the Wigner representation," Phys. Rev. A **54**, 4752 (1996).

[12] J. Hilgevoord, "Time in quantum mechanics," Am. J. Phys. **70**, 301 (2002).

[13] H. Salecker and E. P. Wigner, "Quantum limitations of the measurement of space-time distances," Phys. Rev. **109**, 571 (1958).

[14] A. I. Baz', "Lifetime of intermediate states," Sov. J. Nucl. Phys. **4**, 182 (1967).

[15] V. F. Rybachenko, "Time of penetration of a particle through a potential barrier," Sov. J. Nucl. Phys. **5**, 635 (1967).

[16] A. Peres, "Measurement of time by quantum clocks," Am. J. Phys. **48**, 552 (1980).

[17] M. Büttiker, "Larmor precession and the traversal time for tunneling," Phys. Rev. B **27**, 6178 (1983).

[18] P. A. Martin and M. Sassoli de Bianchi, "On the theory of the Larmor clock and time delay," J. Phys. A: Math. Gen. **25**, 3627 (1992).

[19] M. Büttiker and R. Landauer, "Traversal time for tunneling," Phys. Rev. Lett. **49**, 1739 (1982).

[20] M. Büttiker and R. Landauer, "Traversal time for tunneling," Physica Scripta **32**, 429 (1985).

[21] P. Eckle, M. Smolarski, P. Schlup, J. Biegert, A. Staudte, M. Schöffler, H. G. Muller, R. Dörner, and U. Keller, "Attosecond angular streaking," Nat. Phys. **4**, 565 (2008).

[22] P. Eckle, A. N. Pfeiffer, C. Cirelli, A. Staudte, R. Dörner, H. G. Muller, M. Büttiker, and U. Keller, "Attosecond ionization and tunneling delay time measurements in helium," Science **322**, 1525 (2008).

[23] Y. Ban, E. Y. Sherman, J. G. Muga, and M. Büttiker, "Time scales of tunneling decay of a localized state," Phys. Rev. A **82**, 062121 (2010).

[24] G. Orlando, C. R. McDonald, N. H. Protik, G. Vampa, and T. Brabec, "Tunnelling time, what does it mean?" J. Phys. B: At., Mol. Opt. Phys. **47**, 204002 (2014).

[25] L. V. Keldysh, "Ionization in the field of a strong electromagnetic wave," Sov. Phys.-JETP **20**, 1307 (1965).

[26] M. Lein, "Streaking analysis of strong-field ionisation," J. Mod. Opt. **58**, 1188 (2011).

[27] E. Yakaboylu, M. Klaiber, H. Bauke, K. Z. Hatsagortsyan, and C. H. Keitel, "Relativistic features and time delay of laser-induced tunnel ionization," Phys. Rev. A **88**, 063421 (2013).

[28] C. R. McDonald, G. Orlando, G. Vampa, and T. Brabec, "Tunnel ionization dynamics of bound systems in laser fields: How long does it take for a bound electron to tunnel?" Phys. Rev. Lett. **111**, 090405 (2013).

[29] M. Klaiber, E. Yakaboylu, H. Bauke, K. Z. Hatsagortsyan, and C. H. Keitel, "Under-the-barrier dynamics in laser-induced relativistic tunneling," Phys. Rev. Lett. **110**, 153004 (2013).

[30] J. Zhao and M. Lein, "Determination of ionization and tunneling times in high-order harmonic generation," Phys. Rev. Lett. **111**, 043901 (2013).

[31] J. Kaushal and O. Smirnova, "Nonadiabatic Coulomb effects in strong-field ionization in circularly polarized laser fields," Phys. Rev. A **88**, 013421 (2013).

[32] A. S. Landsman, M. Weger, J. Maurer, R. Boge, A. Ludwig, S. Heuser, C. Cirelli, L. Gallmann, and U. Keller, "Ultrafast resolution of tunneling delay time," Optica **1**, 343 (2014).

[33] E. Yakaboylu, M. Klaiber, and K. Z. Hatsagortsyan, "Wigner time delay for tunneling ionization via the electron propagator," Phys. Rev. A **90**, 012116 (2014).

[34] A. Maquet, J. Caillat, and R. Taïeb, "Attosecond delays in photoionization: time and quantum mechanics," J. Phys. B: At., Mol. Opt. Phys. **47**, 204004 (2014).

[35] A. S. Landsman and U. Keller, "Attosecond science and the tunnelling time problem," Phys. Rep. **547**, 1 (2015).

[36] L. Torlina, F. Morales, J. Kaushal, I. Ivanov, A. Kheifets, A. Zielinski, A. Scrinzi, H. G. Muller, S. Sukiasyan, M. Ivanov, and O. Smirnova, "Interpreting attoclock measurements of tunnelling times," Nat. Phys. **11**, 503 (2015).

[37] M. Klaiber, K. Z. Hatsagortsyan, and C. H. Keitel, "Tunneling dynamics in multiphoton ionization and attoclock calibration," Phys. Rev. Lett. **114**, 083001 (2015).

[38] N. Teeny, E. Yakaboylu, H. Bauke, and C. H. Keitel, "Ionization time and exit momentum in strong-field tunnel ionization," Phys. Rev. Lett. **116**, 063003 (2016).

[39] N. Teeny, C. H. Keitel, and H. Bauke, "Virtual-detector approach to tunnel ionization and tunneling times," Phys. Rev. A **94**, 022104 (2016).

[40] E. P. Wigner, "Lower limit for the energy derivative of the scattering phase shift," Phys. Rev. **98**, 145 (1955).

[41] F. T. Smith, "Lifetime matrix in collision theory," Phys. Rev. **118**, 349 (1960).

[42] T. Zimmermann, S. Mishra, B. R. Doran, D. F. Gordon, and A. S. Landsman, "Tunneling time and weak measurement in strong field ionization," Phys. Rev. Lett. **116**, 233603 (2016).

[43] E. Hewitt and R. E. Hewitt, "The Gibbs-Wilbraham phenomenon: An episode in fourier analysis," Archive for History of Exact Sciences **21**, 129 (1979).

[44] C. R. Leavens, "Application of the quantum clock of Salecker and Wigner to the "tunneling time problem"," Solid State Commun. **86**, 781 (1993).

[45] C. R. Leavens, "Transmission, reflection and dwell times within Bohm's causal interpretation of quantum mechanics," Solid State Commun. **74**, 923 (1990).

[46] V. S. Olkhovsky and E. Recami, "Recent developments in the time analysis of tunneling processes," Phys. Rep. **214**, 339 (1992).

[47] A. M. Steinberg, "How much time does a tunneling particle spend in the barrier region?" Phys. Rev. Lett. **74**, 2405 (1995).

[48] J. Muga, S. Brouard, and R. Sala, "Transmission and reflection tunneling times," Phys. Lett. A **167**, 24 (1992).

[49] C. R. Leavens, "The "tunneling time problem": fundamental incompatibility of the Bohm trajectory approach with the projector and conventional probability current approaches," Phys. Lett. A **197**, 88 (1995).

[50] M. Goto, H. Iwamoto, V. M. d. Aquino, V. C. Aguilera-Navarro,

and D. H. Kobe, "Relationship between dwell, transmission and reflection tunnelling times," J. Phys. A: Math. Gen. **37**, 3599 (2004).

[51] X. L. Yang, S. H. Guo, F. T. Chan, K. W. Wong, and W. Y. Ching, "Analytic solution of a two-dimensional hydrogen atom. I. Nonrelativistic theory," Phys. Rev. A **43**, 1186 (1991).

[52] G. Orlando, C. R. McDonald, N. H. Protik, and T. Brabec, "Identification of the Keldysh time as a lower limit for the tunneling time," Phys. Rev. A **89**, 014102 (2014).

[53] M. Suzuki, "Generalized Trotter´s formula and systematic approximants of exponential operators and inner derivations with applications to many-body problems," Commun. Math. Phys. **51**, 183 (1976).

[54] T. J. Park and J. C. Light, "Unitary quantum time evolution by iterative Lanczos reduction," J. Chem. Phys. **85**, 5870 (1986).

[55] R. Beerwerth and H. Bauke, "Krylov subspace methods for the Dirac equation," Comp. Phys. Comm. **188**, 189 (2015).